



Intravoxel incoherent motion magnetic resonance imaging in assessing histopathological features of gastric cancers: initial findings

Changfeng Ji^{1*}, Ling Chen^{2*}, Wenxian Guan³, Tingting Guo⁴, Qinglei Zhang¹, Song Liu¹, Jian He¹, Zhengyang Zhou¹

¹Department of Radiology, ²Department of Pathology, ³Department of Gastrointestinal Surgery, Nanjing Drum Tower Hospital, The Affiliated Hospital of Nanjing University Medical School, Nanjing 210008, China; ⁴Department of Radiology, Nanjing Drum Tower Hospital, Clinical College of Traditional Chinese and Western Medicine, Nanjing University of Chinese Medicine, Nanjing 210008, China

Contributions: (I) Conception and design: S Liu, J He, Z Zhou; (II) Administrative support: Z Zhou; (III) Provision of study materials or patients: L Chen, W Guan; (IV) Collection and assembly of data: C Ji, T Guo, Q Zhang; (V) Data analysis and interpretation: C Ji, L Chen, S Liu; (VI) Manuscript writing: All authors; (VII) Final approval of manuscript: All authors.

*These authors contributed equally to this work.

Correspondence to: Song Liu, MD. No. 321 Zhongshan Road, Nanjing 210008, China. Email: liusongnj@126.com; Jian He, MD, PhD. No. 321 Zhongshan Road, Nanjing 210008, China. Email: hjxueren@126.com; Zhengyang Zhou, MD, PhD. No. 321 Zhongshan Road, Nanjing 210008, China. Email: zyzhou@nju.edu.cn.

Background: Intravoxel incoherent motion (IVIM) magnetic resonance (MR) imaging has been widely utilized in evaluating various tumors. The application of IVIM MR imaging in characterizing gastric cancer's histopathological features has never been reported previously.

Methods: A total of 62 patients with gastric cancers were prospectively enrolled in this study. All patients underwent MR examination before surgery. All MR images were reviewed by 2 radiologists using software IDL 6.3 and an oval region of interest (ROI) was manually drawn on the specific slice showing the largest area of tumor. Four parameters were calculated automatically: apparent diffusion coefficient (ADC), pure diffusion coefficient (D), perfusion related fraction (f) and pseudo diffusion coefficient (D*). One-way analysis of variance (normality) or Kruskal-Wallis test (non-normality), independent samples *t*-test (normality) or Mann-Whitney U test (non-normality), Spearman correlation test and receiver operating characteristic (ROC) curve analysis were used for statistical analyses.

Results: Poorly/moderate-poorly differentiated gastric cancers showed significantly lower ADC and D values compared with moderately/well differentiated tumors ($P=0.001$, $P<0.001$, respectively). Significant differences were also observed for ADC and D values among different Lauren classifications ($P=0.004$, 0.048 , respectively). No significant differences were observed for f and D* values among different differentiation degrees ($P=0.774$, 0.716 , respectively) and Lauren classifications ($P=0.633$, 0.290 , respectively). The ADC and D values correlated negatively with T stage ($r=-0.363$, -0.295 , respectively), N stage ($r=-0.265$, -0.285 , respectively) and overall stage ($r=-0.485$, -0.368 , respectively) of gastric cancers, but no significant correlations were observed for f and D* values (all $P>0.05$). No significant differences were found for ADC, D, f or D* values among different status of vascular invasion and perineural invasion.

Conclusions: The IVIM-derived ADC and D values showed significant differences among different histological differentiation, Lauren classification and TNM stage of gastric cancers. They showed potential in assessing gastric cancer's histopathological features.

Keywords: Histopathological features; intravoxel incoherent motion (IVIM); magnetic resonance (MR) imaging; stomach neoplasm

Submitted Sep 12, 2017. Accepted for publication Nov 07, 2017.

doi: 10.21037/tcr.2017.11.15

View this article at: <http://dx.doi.org/10.21037/tcr.2017.11.15>

Introduction

Gastric cancer is a common gastrointestinal malignancy, with high morbidity and mortality worldwide (1). Prognosis and treatment strategies of gastric cancers are influenced by histopathological features including histological differentiation, Lauren classification, TNM stage, the status of vascular and perineural invasion, etc. (2-5). Thus, the preoperative assessing of those features is regarded as considerable. As a conventional tool to acquire histopathological features of gastric cancers, endoscopic biopsy involves an invasive procedure relying on the operator's experience and is unable to avoid sampling error (6,7). CT is a common imaging modality for preoperative staging of gastric cancer, yet it could provide little information about histopathology.

As a noninvasive examination with outstanding soft-tissue contrast superior to CT, magnetic resonance (MR) imaging proved useful in the assessment of gastric cancers. And diffusion weighted (DW) MR imaging has shown great potential in differential diagnosis, preoperative staging and characterization of gastric cancers (8-12). For instance, the apparent diffusion coefficient (ADC) values showed significant correlations with differentiation degree, Lauren classification, and even human epidermal growth factor receptor-2 (HER2) status of gastric cancers in our previous studies (13-15).

Nevertheless, the ADC value of gastric cancer was calculated from a simple mono-exponential decay model, which reflects a combination effect of both water molecular diffusion and microvascular perfusion (16). Since the gastric cancer is rich of blood supply, the perfusion component might have a great influence on the measurement of ADC values. As an extended method based on DWI, intravoxel incoherent motion (IVIM) is able to separate diffusion from perfusion component *in vivo* by using an increased number of b values (17). MR signals obtained at lower b values are mainly related to perfusion, while diffusion effects display dominance at higher b values (18). By using a bi-exponential decay model, the pure diffusion coefficient (D) and pseudo diffusion coefficient (D*) could be obtained simultaneously, along with perfusion related fraction (f). Since its first introduction in 1986 (19), IVIM MR imaging has been widely utilized in evaluating various tumors and hepatic fibrosis

(20-25). In our previous study, we confirmed the feasibility of ADC and D values in preoperative assessment of HER2 status of gastric cancers (26). Furthermore, several studies have also confirmed that IVIM is superior to traditional DWI for characterizing malignancy potential of tumors. For instance, Woo *et al.* reported that the D value showed a higher accuracy than ADC value in differentiating high-grade hepatocellular carcinomas from low-grade ones (27). Kang *et al.* demonstrated that D* and f were more valuable parameters in identifying pancreatic adenocarcinomas from neuroendocrine tumors than ADC (28).

However, to the best of our knowledge, the application of IVIM MR imaging in characterizing gastric cancer's histopathological features has never been reported previously. Thus, the purpose of this study was to evaluate the potential associations between parameters derived from IVIM and the histopathological features of gastric cancers.

Methods

Patients

Our study received the approval of local ethics committee. Written informed consent was obtained from each patient. Patients who satisfied the following criteria were potentially included in this study: (I) with a diagnosis of gastric cancer confirmed by endoscopic biopsy; (II) willing to undergo MR examination for preoperative assessment; (III) without absolute contraindications to MR examination and gadolinium contrast agents, such as cardiac pacemaker or defibrillator, aneurysm clip, insulin pump, nerve stimulator, cochlear implant. The exclusion criteria were as follows: (I) receiving local or systematic treatment before MR examination or surgery; (II) without accurate postoperative histopathological information (including differentiation degree, Lauren classification, TNM stage, vascular and perineural invasion); (III) with a minimum diameter of tumor less than 5 mm insufficient to contain a region of interest (ROI); (IV) poor MR image quality for further analysis due to motion or magnetic susceptibility artifacts.

From Nov. 2015 to Dec. 2016, a total of 62 patients (35 men, 27 women) with a mean age of 62±10 years (range, 28–84 years) were prospectively enrolled in this study. A detailed inclusion and exclusion flowchart is shown in *Figure 1*.

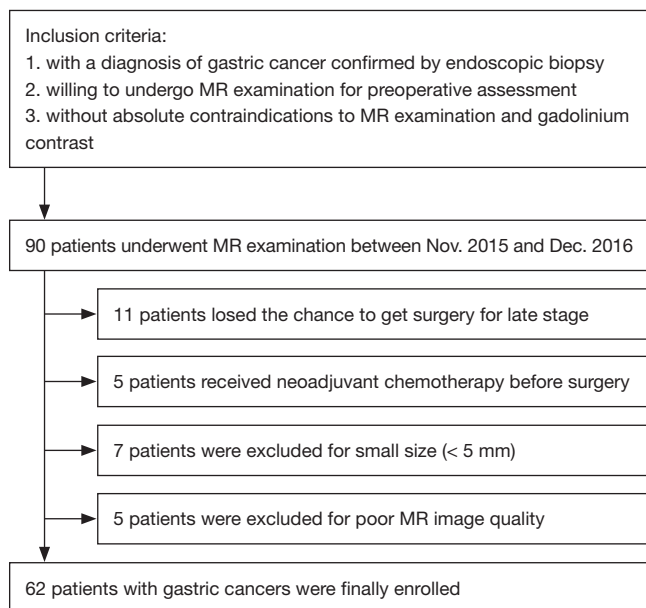


Figure 1 Inclusion and exclusion flowchart of this study. MR, magnetic resonance.

MR examination

All patients underwent MR examination after fasting over 8 hours. After confirming that no contraindications (such as glaucoma, prostate hypertrophy or severe heart disease) were presented, 20 mg of scopolamine butylbromide (1 mL: 20 mg; Chengdu NO.1 Drug Research Institute Company Limited, Chengdu, China) was injected intramuscularly to prevent gastrointestinal motility 10 minutes before MR examination. Fifty-three (85.5%) of 62 patients received scopolamine butylbromide (no adverse effects occurred during and after MR examination), whereas the remaining 9 patients (14.5%) had a contradiction to the drug regimen (7 patients) or refused to use the drug (2 patients). Furthermore, all patients were asked to drink 800–1,000 mL warm water 10 minutes before MR examination to fill the gastric cavity. Before MR scanning, the patients were also trained to breathe smoothly.

All MR images were collected by using a clinical whole body 3.0 T scanner (Ingenia 3.0 T; Philips Medical Systems, Best, the Netherlands) with a 32 channels dStream Torso coil. Patients were placed in a supine position with head first. The respiratory sensor was carefully placed between the patient and coil. Scan duration per respiration and respiratory trigger delay were fit into the expiration phase of each patient's respiratory cycle. The maximum gradient

strength and slew rate of the MR scanner system were 45 mT/s and 200 mT/m/s, respectively.

Axial respiratory-triggered single-shot echo-planar IVIM sequence used b values of 0, 25, 50, 75, 100, 150, 200, 500, 800 s/mm². Although more and higher b values might provide more data for estimating IVIM-related parameters (29), it required longer scanning time. Therefore, a total of 9 b values with 6 b values lower than 200 s/mm² were adopted in our study according to Koh *et al.*'s recommendation (30). And the numbers of signal averages were one average (b value of 0–199 s/mm²), two averages (b value of 200–499 s/mm²) and four averages (b value of 500–800 s/mm²). Other detailed parameters of IVIM sequence were as follows: repetition time = 2,628 ms, echo time = 55 ms, slice thickness = 5 mm, slice gap = 0.5 mm, field of view = 360×300 mm², matrix = 116×100, parallel imaging factor = 4 and bandwidth = 2,666.6 Hz/pixel. The spectral presaturation with inversion recovery fat suppression technique was used for IVIM sequence. There were three motion probe gradient directions, which were frequency encoding, phase encoding and slice choosing directions, respectively. Other sequences included axial T2 weighted (T2W) imaging and axial multiphase enhanced T1 high resolution isotropic volume excitation (THRIVE).

T2W images were obtained with respiratory-triggered turbo spin-echo sequence without fat-saturation (repetition time = 1,000 ms, echo time = 80 ms, field of view = 380×380 mm², matrix = 308×252, slice thickness = 5 mm, slice gap = 0.5 mm, number of signal averages = 2 and bandwidth = 534.0 Hz/pixel).

THRIVE with breath-holding and spectral attenuated inversion recovery techniques (repetition time = 3.00 ms, echo time = 1.42 ms, field of view = 380×380 mm², matrix = 224×194, slice thickness = 5 mm, slice gap = 0.5 mm, number of signal averaged = 1 and bandwidth = 715.4 Hz/pixel) were utilized before and 30, 60, 90, and 180 s after administration of 0.2 mL per kilogram of body weight gadodiamide (Omniscan 0.5 mmol/mL; GE Healthcare, Ireland) using an automatic power injector (Medrad Spectris Solaris EP MR Injector System; One Medrad Drive Indianola, PA, USA).

Image analyses

All MR images were reviewed by 2 radiologists with 8- and 10-year experience in abdominal radiology, who were blinded to the endoscopic biopsy and postoperative pathological findings.

The IVIM sequence was loaded into a software IDL 6.3

(ITT Visual Information Solutions, Boulder, USA), and then was analyzed automatically with mono-exponential and bi-exponential models introduced by Le Bihan (17). The ADC value was calculated by using all the 9 b values (0–800 s/mm^2) fitted to a mono-exponential decay model: $S_b/S_0 = \exp(-b \times \text{ADC})$. The D , f and D^* values were calculated by a bi-exponential model, using segmented fitting method with a threshold b value of 200 s/mm^2 . Equation One: $S_b/S_0 = (1-f) \times \exp(-b \times D) + f \times \exp(-b \times D^*)$, in which S_b is the signal intensity at a certain b value and S_0 is the signal intensity at a b value of 0 s/mm^2 . Because D^* is roughly one order of magnitude greater than D , $-b \times D^*$ is less than -3 at a high b value ($>200 \text{ s}/\text{mm}^2$) and $f \times \exp(-b \times D^*)$ is less than $0.05 f$. In this case, the contribution of D^* to the S_b/S_0 signal ratio can be ignored, and Equation One can be simplified to Equation Two to estimate D : $S_b/S_0 = \exp(-b \times D)$. Thus, for the high b values (larger than 200 s/mm^2), S_b was first fitted to Equation Two with a linear model, and D was calculated. Then, the f and D^* coefficients were computed using Equation One for all b values considering the calculated D values by a nonlinear Levenberg-Marquardt method.

Considering the solid part of tumors *in vitro* was always selected for pathological analyses, we set the ROIs within the solid part of lesions on MR imaging. Gastric cancer showed thickened wall on T2W images, and the solid part showed hyperintense on IVIM ($b=800 \text{ s}/\text{mm}^2$) with remarkable contrast enhancement. For each patient, the specific slice of axial IVIM image ($b=800 \text{ s}/\text{mm}^2$) showing the largest area of tumor was selected. Based on the consensus of two radiologists, an oval ROI was manually drawn as large as possible within the solid part of the lesion by referring to the corresponding images of other MR sequences. If the lesion showed a sandwich sign (12), the ROI was set to avoid the internal muscular layer. Regions with necrosis or artifact were also carefully kept away. In our study, there were 10 lesions (16.1%) showing macroscopic necrosis based on MR images (hypointense on T1W images, hyperintense on T2W images, without contrast enhancement). The mean volume of the necrotic areas was $2,503.0 \pm 1,461.1 \text{ mm}^3$, which accounted for 4.3% of the whole tumor volume. Then the ROI was automatically transferred into the parameter maps and the mean values from the ROI were obtained.

Postoperative histopathological analyses

Fifty-three patients underwent curative gastrectomy (including 24 total and 29 partial gastrectomies) and 9

patients underwent palliative resection by the surgeons with 6- and 9-year experience in gastrointestinal surgery. The pathological analyses were performed by a pathologist with 6-year experience in digestive malignancy, who was blinded to MR findings and IVIM measurements. The histological differentiation, Lauren classification, vascular invasion, perineural invasion and TNM stage of the gastric cancers were analyzed and recorded according to the World Health Organization (WHO) classification [2010] and the TNM classification of the American Joint Committee on Cancer (AJCC, 7th edition) (31,32).

Statistical analyses

Shapiro-Wilk tests were used to check normality assumption for all parameters in all groups ($P < 0.05$ indicates non-normal distribution). Quantitative values in normal distribution were presented as mean \pm standard deviation, while those in non-normal distribution were presented as median (interquartile range).

One-way analysis of variance (normality) or Kruskal-Wallis test (non-normality) were used to detect the difference of the ADC, D , f and D^* values among different Lauren classifications and T stages. Independent samples t -test (normality) or Mann-Whitney U test (non-normality) were used for comparison of ADC, D , f and D^* values between different differentiation degrees (poorly/moderate-poorly *vs.* moderately/well), N stages (N0 *vs.* N1–3), overall stages (I–II *vs.* III–IV), vascular invasion (absent *vs.* present) and perineural invasion (absent *vs.* present).

Diagnostic performance of the ADC, D , f and D^* values in differentiating gastric cancers with poor differentiation degree (poorly/moderate-poorly), diffuse type, lymph node metastasis, vascular or perineural invasion was tested with receiver operating characteristic (ROC) curve analysis. The cutoff values with the largest Youden index (sensitivity + specificity – 1) were calculated from the ROC curves. We also made multivariate regression analyses to differentiate poorly/moderate-poorly from moderately/well differentiated gastric cancers.

Correlations between ADC, D , f and D^* values with differentiation degree, Lauren classification, T stage, N stage and overall stage of gastric cancers were evaluated with Spearman correlation test (correlation coefficient r , 0.000–0.199, very weak; 0.200–0.399, weak; 0.400–0.599, moderate; 0.600–0.799, strong; 0.800–1.000, very strong) (33).

ROC curve analysis was performed with MedCalc Statistical Software (version 11.4.2.0, MedCalc Software

Table 1 The clinicopathological characteristics of the patients with gastric cancers

Characteristics	No. of patients	Percentage (%)
Gender		
Male	38	61.3
Female	24	38.7
Age		
<60 years	20	32.3
≥60 years	42	67.7
Location		
Cardia	18	29.0
Body	15	24.2
Antrum	21	33.9
Cardia + body	2	3.2
Body + antrum	3	4.8
Cardia + body + antrum	3	4.8
Pathological type		
Ade	43	69.4
Pcc	11	17.7
Muc	2	3.2
Ade + Pcc	3	4.8
Ade + Muc	1	1.6
Pcc + Muc	2	3.2
Differentiation degree		
Poorly	35	56.5
Moderate-poorly	17	27.4
Moderately	8	12.9
Well	2	3.2
Lauren classification		
Diffuse	26	41.9
Mixed	15	24.2
Intestinal	21	33.9
T stage		
T1	6	9.7
T2	8	12.9
T3	35	56.5
T4	13	21.0

Table 1 (continued)

Table 1 (continued)

Characteristics	No. of patients	Percentage (%)
N stage		
N0	11	17.7
N1	9	14.5
N2	17	27.4
N3	25	40.3
Overall stage		
I	6	9.7
II	11	17.7
III	41	66.1
IV	4	6.5
Lymph node metastasis		
Absent	11	17.7
Present	51	82.3
Vascular invasion		
Absent	11	17.7
Present	51	82.3
Perineural invasion		
Absent	16	25.8
Present	46	74.2

bvba) and other statistical analyses were performed with SPSS (version 22.0 for Microsoft Windows x64, SPSS, US). A two-tailed P value less than 0.05 was considered statistically significant.

Results

The clinicopathological characteristics of all the 62 patients with gastric cancers were shown in *Table 1*. Each patient had one lesion identified. A representative case of gastric cancer was shown in *Figure 2*.

Differences Tests

According to Shapiro-Wilk tests, the P values of ADC, D, f and D* values in all groups were shown in *Table S1*.

There were lower ADC and D values for poorly/moderate-poorly differentiated gastric cancers compared with moderately/well differentiated tumors. Significant

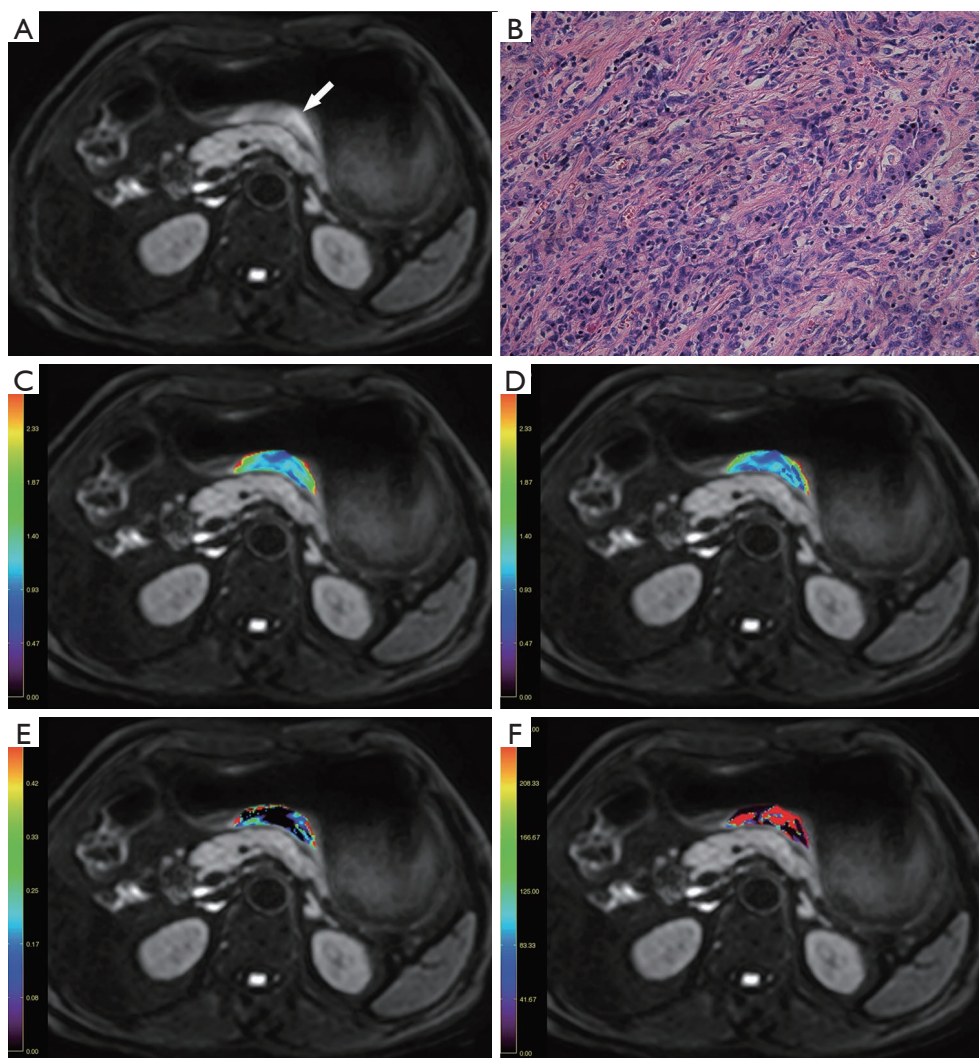


Figure 2 A 73-year-old man with gastric cancer pathologically diagnosed at stage T4N2. (A) Axial intravoxel incoherent motion (IVIM) magnetic resonance (MR) image ($b = 800 \text{ s/mm}^2$) shows a thickened wall in stomach body (white arrow) with remarkably high signal intensity; (B) the photomicrograph (Hematoxylin & Eosin staining, $\times 400$) shows a poorly cohesive carcinoma with a Lauren classification of diffuse type, the corresponding (C) apparent diffusion coefficient (ADC); (D) pure diffusion coefficient (D); (E) perfusion related fraction (f); and (F) pseudo diffusion coefficient (D^*) maps fused with (A) show that this lesion has an ADC value of $1.187 \times 10^{-3} \text{ mm}^2/\text{s}$, a D value of $1.112 \times 10^{-3} \text{ mm}^2/\text{s}$, a f value of 0.064 and a D^* value of $33.686 \text{ mm}^2/\text{s}$, respectively.

differences were also observed for ADC and D values among different Lauren classifications. Diffuse type tumors showed lower ADC and D values. There were also lower ADC and D values for gastric cancers with III-IV stages, and those with lymph node metastasis, while only ADC values showed differences among different T stages. No significant differences were found for ADC, D, f or D^* values among different status of vascular invasion and perineural invasion (Table 2).

ROC curve analysis

ADC and D values performed well in differentiate poorly/moderate-poorly differentiated gastric cancers from moderately/well differentiated ones with an area under the ROC curve (AUC) of 0.810 and 0.830, respectively. They could also differentiate gastric cancers with or without lymph node metastasis, and the AUC for them were 0.800 and 0.727, respectively. Only ADC value could differentiate

Table 2 The apparent diffusion coefficient (ADC), pure diffusion coefficient (D), perfusion related fraction (f) and pseudo diffusion coefficient (D*) values of gastric cancers with different histopathological features

Histopathological features	ADC	D	f	D*
Differentiation degree				
Poorly/moderate-poorly	1.320±0.259	1.039±0.215	0.160 (0.167)	30.127 (37.101)
Moderately/well	1.649±0.282	1.351±0.239	0.153 (0.062)	22.497 (35.711)
I-S test or M-W test	0.001 [†]	<0.001 [†]	0.774	0.716
Lauren classification				
Diffuse	1.187 (0.264)	1.024±0.218	0.146 (0.145)	25.401 (39.436)
Mixed	1.339 (0.413)	1.056±0.249	0.172 (0.199)	42.681 (74.686)
Intestinal	1.616 (0.467)	1.194±0.252	0.164 (0.153)	22.426 (26.084)
ANOVA or K-M test	0.004 [‡]	0.048 [‡]	0.633	0.290
T stage				
T1	1.629 (0.218)	1.262±0.249	0.222 (0.154)	21.546 (62.076)
T2	1.451 (0.485)	1.186±0.243	0.160 (0.180)	31.509 (45.564)
T3	1.339 (0.421)	1.068±0.237	0.146 (0.140)	35.050 (46.818)
T4	1.151 (0.410)	1.008±0.242	0.160 (0.191)	15.943 (24.156)
ANOVA or K-M test	0.023 [‡]	0.115	0.571	0.081
N stage				
N0	1.624±0.212	1.249±0.227	0.201 (0.144)	16.577 (36.430)
N1-3	1.319±0.273	1.055±0.238	0.157 (0.166)	28.655 (36.167)
I-S test or M-W test	0.001 [†]	0.016 [†]	0.214	0.456
Overall stage				
I-II	1.557±0.316	1.200±0.225	0.189 (0.155)	18.817 (35.870)
III-IV	1.304±0.245	1.047±0.243	0.172 (0.158)	28.655 (36.704)
I-S test or M-W test	0.001 [†]	0.029 [†]	0.421	0.630
Vascular invasion				
Absent	1.414 (0.489)	1.109±0.292	0.195 (0.133)	16.577 (41.074)
Present	1.348 (0.429)	1.085±0.238	0.159 (0.165)	28.655 (33.149)
I-S test or M-W test	0.434	0.769	0.562	0.525
Perineural invasion				
Absent	1.412 (0.508)	1.130±0.276	0.143 (0.139)	36.449 (33.575)
Present	1.345 (0.438)	1.075±0.236	0.164 (0.165)	22.542 (37.298)
I-S test or M-W test	0.450	0.440	0.499	0.735

The values of ADC, D, f and D* in normal distribution were presented as mean ± standard deviation, while those in non-normal distribution were presented as median (interquartile range), according to Shapiro-Wilk tests (P<0.05 indicates non-normal distribution). [†], P<0.05 with independent samples *t*-test (normality) or Mann-Whitney U test (non-normality); [‡], P<0.05 with one-way analysis of variance (normality) or Kruskal-Wallis test (non-normality). The ADC, D and D* values are in unit of × 10⁻³ mm²/s. Ade, tubular or papillary adenocarcinoma; Pcc, poorly cohesive carcinoma; I-S test, independent samples *t*-test; M-W test, Mann-Whitney U test; ANOVA, one-way analysis of variance; K-M test, Kruskal-Wallis test.

Table 3 Diagnostic performance of the apparent diffusion coefficient (ADC), pure diffusion coefficient (D), perfusion related fraction (f) and pseudo diffusion coefficient (D*) values with receiver operating characteristic (ROC) curve analysis

Types	Parameters	Cut-off	Sensitivity (%)	Specificity (%)	AUC	P value
Poorly/moderate-poorly	ADC	1.369	65.4	90.0	0.810	<0.001 [†]
	D	1.147	71.2	90.0	0.830	<0.001 [†]
	f	0.167	48.1	80.0	0.529	0.741
	D*	32.276	48.1	70.0	0.537	0.699
Diffuse type	ADC	1.356	73.1	63.9	0.682	0.008 [†]
	D	1.112	76.9	55.6	0.634	0.063
	f	0.160	61.5	55.6	0.529	0.702
	D*	14.388	38.5	80.6	0.550	0.513
Lymph node metastasis	ADC	1.558	82.4	72.7	0.800	< 0.001 [†]
	D	1.005	47.1	90.9	0.727	0.003 [†]
	f	0.139	41.2	90.9	0.620	0.172
	D*	16.577	68.6	54.5	0.572	0.497
Vascular invasion	ADC	1.558	76.5	45.5	0.576	0.447
	D	1.052	51.0	63.6	0.529	0.780
	f	0.189	66.7	54.5	0.556	0.562
	D*	16.577	68.6	54.5	0.561	0.579
Perineural invasion	ADC	1.190	43.5	75.0	0.564	0.472
	D	1.348	93.5	25.0	0.553	0.559
	f	0.164	50.0	68.7	0.557	0.510
	D*	36.992	67.4	50.0	0.529	0.740

The ADC, D and D* values are in unit of $\times 10^{-3} \text{ mm}^2/\text{s}$. [†], P<0.05 with ROC curve analysis. AUC, area under the ROC curve.

gastric cancers with diffuse type from those with mixed and intestinal types with an AUC of 0.682 (Table 3, Figure 3). Based on multivariable model, ADC combined with D values showed an AUC of 0.846 in differentiating poorly/moderate-poorly from moderately/well differentiated gastric cancers.

Spearman correlation test

Both ADC and D values correlated positively with differentiation degree ($r=0.421$, 0.354 , respectively) and Lauren classification ($r=0.400$, 0.282 , respectively) of gastric cancers. They also correlated negatively with T stages ($r=-0.363$, -0.295 , respectively), N stages ($r=-0.265$, -0.285 , respectively) and overall stages ($r=-0.485$, -0.368 , respectively) of gastric cancers. No significant correlations

were found between f and D* values with histopathological features of gastric cancers (Table 4).

Discussion

We confirmed the feasibility of IVIM MR imaging in characterizing and predicting histopathological features of gastric cancers, which has never been reported previously. To the best of our knowledge, there was no modality except endoscopic biopsy to obtain the histopathological information of gastric cancers preoperatively. And it was sometimes difficult to make an accurate assessment of differentiation degree and Lauren classification based on a patch of specimen through biopsy. Lee *et al.* reported that in 285 of 1,326 patients (21.5%) with gastric cancers, the differentiation degree determined based on preoperative

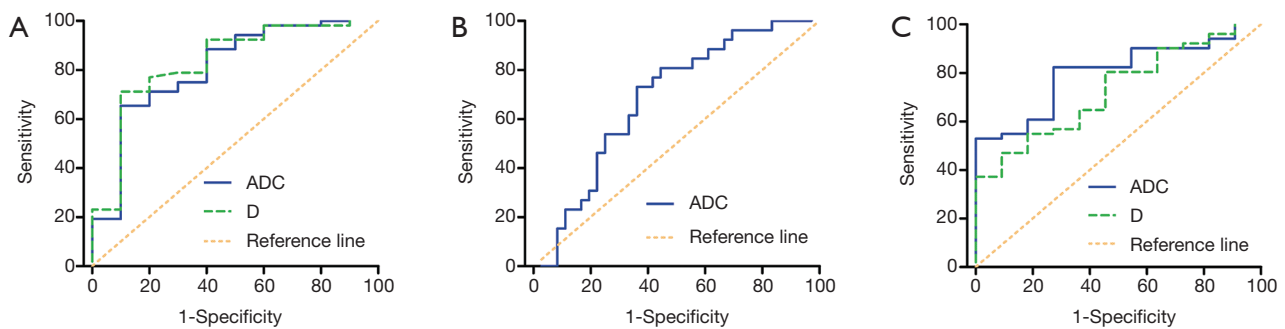


Figure 3 Graphs showing the diagnostic performance of the apparent diffusion coefficient (ADC) and pure diffusion coefficient (D) values with receiver operating characteristic (ROC) curve analysis. (A) ROC curves of the ADC and D values in differentiating poorly/moderate-poorly differentiated gastric cancers from moderately/well differentiated ones (area under the ROC curve, AUC =0.810, 0.830, respectively, both P<0.05); (B) ROC curve of the ADC value in differentiating gastric cancers with diffuse type from mixed or intestinal type (AUC =0.682, P<0.05); (C) ROC curves of the ADC and D values in differentiating gastric cancers with lymph node metastasis from those without lymph node metastasis (AUC =0.800, 0.727, respectively, both P <0.05). The reference line indicates random assignment.

Table 4 Correlations between the apparent diffusion coefficient (ADC), pure diffusion coefficient (D), perfusion related fraction (f) and pseudo diffusion coefficient (D*) values with different histopathological features

Histopathological features	ADC	D	f	D*
Differentiation degree				
r	0.421	0.354	0.128	0.074
P value	0.001 [†]	0.005 [†]	0.320	0.566
Lauren classification				
r	0.400	0.282	0.090	0.005
P value	0.001 [†]	0.027 [†]	0.484	0.970
T stage				
r	-0.363	-0.295	-0.116	0.156
P value	0.004 [†]	0.020 [†]	0.368	0.225
N stage				
r	-0.265	-0.285	0.033	0.109
P value	0.038 [†]	0.025 [†]	0.801	0.399
Overall stage				
r	-0.485	-0.368	-0.140	0.057
P value	<0.001 [†]	0.003 [†]	0.278	0.661

[†], P<0.05 with Spearman correlation test.

endoscopic biopsy was inconsistent with that based on post-gastrectomy specimen (7). Flucke *et al.* reported that preoperative biopsy diagnosed Lauren classification differed

from that of surgical specimen in approximately one quarter of patients with gastric cancers (6).

Our previous study has confirmed the correlations between traditional ADC values calculated with two b values (0 and 1,000 s/mm²) and differentiation degree as well as Lauren classification of gastric cancers (14). In this study, the ADC value was calculated with a simple mono-exponential decay model using all the 9 b values (0–800 s/mm²). The D value was calculated with high b values (larger than 200 s/mm²).

Significant correlations were also found between ADC as well as D values and differentiation degree of gastric cancers. We speculated that as the differentiation degree of gastric cancer decreases, the tumor cell irregularity increases with more disordered arrangement, which resulted in decreased ADC and D values (14). Woo *et al.* reported that as the grade of hepatocellular carcinoma increased (differentiation degree decreased), the ADC and D values decreased significantly (27). Since poorly differentiated gastric cancers showed more aggressive behavior, greater treatment challenge and poorer prognosis (2), it is important to identify gastric cancers with poor differentiation degree preoperatively to optimize treatment strategy and improve the prognosis. In our study, both ADC and D values proved useful in differentiating poorly/moderate-poorly gastric cancers from moderately/well differentiated ones, and the AUC for D value (0.830) was slightly higher than ADC (0.810), which was in line with a previous study in differentiating high-grade and low-grade hepatocellular carcinomas (27). Beyond that, by combining

ADC and D values, the AUC could be further increased to 0.846. Therefore, we believe that IVIM MR imaging made sense in evaluating gastric cancers.

The Lauren classification is widely accepted and employed in evaluating gastric cancers. We found significant differences of ADC and D values among gastric cancers with different Lauren classifications. For gastric cancers with diffuse type, low differentiation degree and obvious cellular atypia are common findings, which may cause narrower and more distorted intercellular spaces to restrain the motion of water molecules. Gastric cancers with intestinal type were characterized by tubular or glandular structures with larger intercellular spaces, resulting in higher ADC and D values (14).

Accurate preoperative staging plays an essential role in optimizing therapeutic approaches for patients with gastric cancers (34). A negative correlation was found between ADC and D values with T stage of gastric cancers, which was similar to our previous study using traditional ADC values (35). As the T stage increased, tumors showed stronger ability of proliferation and invasion with increased cell density and disordered cellular arrangement, leading to more restricted and disordered water molecular diffusion and decreased ADC and D values.

It remains a challenge in accurate preoperative assessment of lymph node metastasis on the basis of morphological criteria. Previous studies reported that accuracy of CT in N staging ranged from 69% to 92% (36,37). And the N staging benefited little from MR imaging without functional sequences. Joo *et al.* reported that DW imaging could increase the sensitivity in detecting lymph node metastasis (38). Our previous study demonstrated the capacity of traditional mean ADC in predicting lymph node metastasis of gastric cancers (35). In this study, both ADC and D values derived from IVIM could also identify gastric cancers with lymph node metastasis (AUC =0.800, 0.727, respectively).

It was not surprising to find that the ADC and D values also correlated negatively with overall stage of gastric cancers, which has a great impact on patients' survival. Giganti *et al.* demonstrated a significant prognostic value of ADC values in patients with gastric cancer (39). We speculated a probable relationship between IVIM-derived parameters and patients' survival, which required further confirmation.

We failed to make any significant findings involving perfusion-related f and D^* values in this study. The parameter f represents the vascular volume fraction within

the tissue. Ma *et al.* reported that dynamic contrast enhanced (DCE) derived V_e and K^{trans} showed differences among Lauren classifications (40). And Joo *et al.* demonstrated a significant correlation between V_e and T stage of gastric cancers (41). However, the relationship between IVIM-derived perfusion-related parameters and DCE-derived parameters was still undetermined. Therefore, the role of f value in the evaluation of gastric cancers remains unknown.

Due to poor signal to noise ratio and technique instability (42), the application of D^* value was always limited. Previous studies on digestive malignancies seldom reported significant findings of D^* values (20,43), whose clinical applications remained undetermined.

There were several limitations in this study. Firstly, the correlations between IVIM-derived parameters and histopathological features of gastric cancers were significant yet moderate or sometimes weak. And the diagnostic performance of ADC and D values were not satisfied in clinical settings. Secondly, the ROIs were simply drawn within the solid part in the largest slice of lesions without rigorous reference to postoperative specimens. We will expand the sample size and try whole-volume analysis in our next study.

In conclusion, the IVIM-derived ADC and D values were significantly correlated with histological differentiation, Lauren classification and TNM stage of gastric cancers. According to those initial findings, we confirmed the potential of IVIM MR imaging in assessing histopathological features of gastric cancers, especially in identifying poorly/moderate-poorly differentiated or diffuse type gastric cancers, and in predicting the status of lymph nodes metastasis.

Acknowledgments

Funding: None.

Footnote

Provenance and Peer Review: This article was commissioned by the Guest Editors (Yi-Xiang J. Wang, Yong Wang) for the series "Translational Imaging in Cancer Patient Care" published in *Translational Cancer Research*. The article has undergone external peer review.

Conflicts of Interest: All authors have completed the ICMJE uniform disclosure form (available at <http://dx.doi.org/10.21037/tcr.2017.11.15>). The series "Translational Imaging in Cancer Patient Care" was commissioned by the

editorial office without any funding or sponsorship. The authors have no other conflicts of interest to declare.

Ethical Statement: The authors are accountable for all aspects of the work in ensuring that questions related to the accuracy or integrity of any part of the work are appropriately investigated and resolved. The study was conducted in accordance with the Declaration of Helsinki (as revised in 2013). This prospective study received the approval of local ethics committee (AF/SC-183-01). Written informed consent was obtained from each patient.

Open Access Statement: This is an Open Access article distributed in accordance with the Creative Commons Attribution-NonCommercial-NoDerivs 4.0 International License (CC BY-NC-ND 4.0), which permits the non-commercial replication and distribution of the article with the strict proviso that no changes or edits are made and the original work is properly cited (including links to both the formal publication through the relevant DOI and the license). See: <https://creativecommons.org/licenses/by-nc-nd/4.0/>.

References

1. Torre LA, Bray F, Siegel RL, et al. Global cancer statistics, 2012. *CA Cancer J Clin* 2015;65:87-108.
2. Zu H, Wang H, Li C, et al. Clinicopathologic characteristics and prognostic value of various histological types in advanced gastric cancer. *Int J Clin Exp Pathol* 2014;7:5692-700.
3. Qiu M, Zhou Y, Zhang X, et al. Lauren classification combined with HER2 status is a better prognostic factor in Chinese gastric cancer patients. *BMC Cancer* 2014;14:823.
4. Röcken C, Behrens HM. Validating the prognostic and discriminating value of the TNM-classification for gastric cancer—a critical appraisal. *Eur J Cancer* 2015;51:577-86.
5. Hwang JE, Hong JY, Kim JE, et al. Prognostic significance of the concomitant existence of lymphovascular and perineural invasion in locally advanced gastric cancer patients who underwent curative gastrectomy and adjuvant chemotherapy. *Jpn J Clin Oncol* 2015;45:541-6.
6. Flucke U, Monig SP, Baldus SE, et al. Differences between biopsy- or specimen-related Lauren and World Health Organization classification in gastric cancer. *World J Surg* 2002;26:137-40.
7. Lee IS, Park YS, Lee JH, et al. Pathologic discordance of differentiation between endoscopic biopsy and postoperative specimen in mucosal gastric adenocarcinomas. *Ann Surg Oncol* 2013;20:4231-7.
8. Shinya S, Sasaki T, Nakagawa Y, et al. The usefulness of diffusion-weighted imaging (DWI) for the detection of gastric cancer. *Hepatogastroenterology* 2007;54:1378-81.
9. Tang L, Sun YS, Li ZY, et al. Diffusion-weighted magnetic resonance imaging in the depiction of gastric cancer: initial experience. *Abdom Radiol (NY)* 2016;41:2-9.
10. Liu S, He J, Guan W, et al. Added value of diffusion-weighted MR imaging to T2-weighted and dynamic contrast-enhanced MR imaging in T staging of gastric cancer. *Clin Imaging* 2014;38:122-8.
11. Liu S, He J, Guan W, et al. Preoperative T staging of gastric cancer: comparison of diffusion- and T2-weighted magnetic resonance imaging. *J Comput Assist Tomogr* 2014;38:544-50.
12. Zhang XP, Tang L, Sun YS, et al. Sandwich sign of Borrmann type 4 gastric cancer on diffusion-weighted magnetic resonance imaging. *Eur J Radiol* 2012;81:2481-6.
13. Zhang Y, Chen J, Liu S, et al. Assessment of histological differentiation in gastric cancers using whole-volume histogram analysis of apparent diffusion coefficient maps. *J Magn Reson Imaging* 2017;45:440-9.
14. Liu S, Guan W, Wang H, et al. Apparent diffusion coefficient value of gastric cancer by diffusion-weighted imaging: correlations with the histological differentiation and Lauren classification. *Eur J Radiol* 2014;83:2122-8.
15. He J, Shi H, Zhou Z, et al. Correlation between apparent diffusion coefficients and HER2 status in gastric cancers: pilot study. *BMC Cancer* 2015;15:749.
16. Mazaheri Y, Afaq A, Rowe DB, et al. Diffusion-weighted magnetic resonance imaging of the prostate: improved robustness with stretched exponential modeling. *J Comput Assist Tomogr* 2012;36:695-703.
17. Le Bihan D, Breton E, Lallemand D, et al. Separation of diffusion and perfusion in intravoxel incoherent motion MR imaging. *Radiology* 1988;168:497-505.
18. Padhani AR, Liu G, Koh DM, et al. Diffusion-weighted magnetic resonance imaging as a cancer biomarker: consensus and recommendations. *Neoplasia* 2009;11:102-25.
19. Le Bihan D, Breton E, Lallemand D, et al. MR imaging of intravoxel incoherent motions: application to diffusion and perfusion in neurologic disorders. *Radiology* 1986;161:401-7.
20. Nougaret S, Vargas HA, Lakhman Y, et al. Intravoxel incoherent motion-derived histogram metrics for assessment of response after combined chemotherapy and radiation therapy in rectal cancer: initial experience and comparison between single-section and volumetric

- analyses. *Radiology* 2016;280:446-54.
21. Zhu L, Zhu L, Shi H, et al. Evaluating early response of cervical cancer under concurrent chemo-radiotherapy by intravoxel incoherent motion MR imaging. *BMC Cancer* 2016;16:79.
 22. Kim Y, Ko K, Kim D, et al. Intravoxel incoherent motion diffusion-weighted MR imaging of breast cancer: association with histopathological features and subtypes. *Br J Radiol* 2016;89:20160140.
 23. Yuan J, Wong OL, Lo GG, et al. Statistical assessment of bi-exponential diffusion weighted imaging signal characteristics induced by intravoxel incoherent motion in malignant breast tumors. *Quant Imaging Med Surg* 2016;6:418-29.
 24. Wang YX, Deng M, Li YT, et al. A combined use of intravoxel incoherent motion mri parameters can differentiate early-stage hepatitis-b fibrotic livers from healthy livers. *SLAS Technol* 2017. [Epub ahead of print].
 25. Li YT, Cercueil JP, Yuan J, et al. Liver intravoxel incoherent motion (IVIM) magnetic resonance imaging: a comprehensive review of published data on normal values and applications for fibrosis and tumor evaluation. *Quant Imaging Med Surg* 2017;7:59-78.
 26. Ji C, Zhang Q, Guan W, et al. Role of intravoxel incoherent motion MR imaging in preoperative assessing HER2 status of gastric cancers. *Oncotarget* 2017;8:49293-302.
 27. Woo S, Lee JM, Yoon JH, et al. Intravoxel incoherent motion diffusion-weighted MR imaging of hepatocellular carcinoma: correlation with enhancement degree and histologic grade. *Radiology* 2014;270:758-67.
 28. Kang KM, Lee JM, Yoon JH, et al. Intravoxel incoherent motion diffusion-weighted MR imaging for characterization of focal pancreatic lesions. *Radiology* 2014;270:444-53.
 29. Koh DM, Blackledge M, Collins DJ, et al. Reproducibility and changes in the apparent diffusion coefficients of solid tumours treated with combretastatin A4 phosphate and bevacizumab in a two-centre phase I clinical trial. *Eur Radiol* 2009;19:2728-38.
 30. Koh DM, Collins DJ, Orton MR. Intravoxel incoherent motion in body diffusion-weighted MRI: reality and challenges. *AJR Am J Roentgenol* 2011;196:1351-61.
 31. Lauwers GY, Carneiro F, Graham DY, et al. Gastric carcinoma. In: Bosman FT, Carneiro F, Hruban RH, Theise ND, editors. *WHO classification of tumors of the digestive system*. Lyon: IARC Press, 2010: 225-7.
 32. Edge SB, Byrd DR, Compton CC, et al. *AJCC cancer staging manual*. 7th ed. New York: Springer, 2010.
 33. Zhu L, Pan Z, Ma Q, et al. Diffusion kurtosis imaging study of rectal adenocarcinoma associated with histopathologic prognostic factors: preliminary findings. *Radiology* 2017;284:66-76.
 34. Fang WL, Huang KH, Chen JH, et al. Comparison of the survival difference between AJCC 6th and 7th editions for gastric cancer patients. *World J Surg* 2011;35:2723-9.
 35. Liu S, Wang H, Guan W, et al. Preoperative apparent diffusion coefficient value of gastric cancer by diffusion-weighted imaging: Correlations with postoperative TNM staging. *J Magn Reson Imaging* 2015;42:837-43.
 36. Chen CY, Hsu JS, Wu DC, et al. Gastric cancer: preoperative local staging with 3D multi-detector row CT--correlation with surgical and histopathologic results. *Radiology* 2007;242:472-82.
 37. Yang DM, Kim HC, Jin W, et al. 64 multidetector-row computed tomography for preoperative evaluation of gastric cancer: histological correlation. *J Comput Assist Tomogr* 2007;31:98-103.
 38. Joo I, Lee JM, Kim JH, et al. Prospective comparison of 3T MRI with diffusion-weighted imaging and MDCT for the preoperative TNM staging of gastric cancer. *J Magn Reson Imaging* 2015;41:814-21.
 39. Giganti F, Orsenigo E, Esposito A, et al. Prognostic role of diffusion-weighted mr imaging for resectable gastric cancer. *Radiology* 2015;276:444-52.
 40. Ma L, Xu X, Zhang M, et al. Dynamic contrast-enhanced MRI of gastric cancer: Correlations of the pharmacokinetic parameters with histological type, Lauren classification, and angiogenesis. *Magn Reson Imaging* 2017;37:27-32.
 41. Joo I, Lee JM, Han JK, et al. Dynamic contrast-enhanced MRI of gastric cancer: Correlation of the perfusion parameters with pathological prognostic factors. *J Magn Reson Imaging* 2015;41:1608-14.
 42. Federau C, Haggmann P, Maeder P, et al. Dependence of brain intravoxel incoherent motion perfusion parameters on the cardiac cycle. *PLoS One* 2013;8:e72856.
 43. Lei J, Tian Y, Zhu SC, et al. Preliminary study of IVIM-DWI and DCE-MRI in early diagnosis of esophageal cancer. *Eur Rev Med Pharmacol Sci* 2015;19:3345-50.

Cite this article as: Ji C, Chen L, Guan W, Guo T, Zhang Q, Liu S, He J, Zhou Z. Intravoxel incoherent motion magnetic resonance imaging in assessing histopathological features of gastric cancers: initial findings. *Transl Cancer Res* 2017;6(6):1129-1140. doi: 10.21037/tcr.2017.11.15

Supplementary

Table S1 Shapiro-Wilk tests' P values for normality assumption of the apparent diffusion coefficient (ADC), pure diffusion coefficient (D), perfusion related fraction (f) and pseudo diffusion coefficient (D*) values among gastric cancers with different histopathological features

Histopathological features	ADC	D	f	D*
Differentiation degree				
Poorly/moderate-poorly	0.100	0.804	0.026 [†]	<0.001 [†]
Moderately/well	0.552	0.781	0.031 [†]	0.088
Lauren classification				
Diffuse	0.014 [†]	0.397	0.046 [†]	<0.001 [†]
Mixed	0.989	0.290	0.237	0.076
Intestinal	0.323	0.735	0.310	0.011 [†]
T stage				
T1	0.402	0.470	0.636	0.019 [†]
T2	0.233	0.513	0.499	0.265
T3	0.553	0.851	0.013 [†]	<0.001 [†]
T4	0.015 [†]	0.145	0.154	0.078
N stage				
N0	0.449	0.625	0.586	0.003 [†]
N1-3	0.085	0.552	0.010 [†]	<0.001 [†]
Overall stage				
I-II	0.187	0.910	0.288	0.002 [†]
II-III	0.060	0.300	0.021 [†]	<0.001 [†]
Vascular invasion				
Absent	0.920	0.884	0.858	0.005 [†]
Present	0.046 [†]	0.641	0.015 [†]	<0.001 [†]
Perineural invasion				
Absent	0.775	0.805	0.185	0.005 [†]
Present	0.008 [†]	0.636	0.042 [†]	<0.001 [†]

[†], P<0.05 indicates non-normal distribution.